

Monolayer Formation of Cytochrome b_{562} on Gold Surfaces and Its Reconstitution Reaction, Studied by Surface Plasmon Resonance Spectroscopy

Kazutoshi Kobayashi,[#] Masafumi Shimizu,[†] Teruyuki Nagamune,[*,†] Hiroyuki Sasabe,[##] Yu Fang,[††] and Wolfgang Knoll[††]

Frontier Research Program, The Institute of Physical and Chemical Research (RIKEN), 2-1 Hirosawa, Wako 351-0198

†Department of Chemistry and Biotechnology, School of Engineering, The University of Tokyo, 7-3-1 Hongo, Bunkyo-ku, Tokyo 113-8656

††Max-Planck-Institut für Polymerforschung, Ackermannweg 10, D-55128 Mainz, Germany

(Received November 28, 2001)

Association and dissociation reactions of cytochrome b_{562} on solid surfaces were investigated by means of surface plasmon resonance spectroscopy. Propionates of side chains in the heme molecule were modified with sulfur moiety as an anchor part to be adsorbed on the gold substrate. This modified heme was firstly reconstituted with apo-protein in solution. This reconstituted holo-protein was then adsorbed on either bare gold substrate or pre-modified gold substrate. Native cytochrome b_{562} was also adsorbed to the same substrates for the control experiment. The reconstituted cytochrome b_{562} was successfully adsorbed on the pre-treated gold substrate without denaturation in structure, probably with homogeneous anisotropic orientation. Guanidine hydrochloride in the buffer of pH 5.0 was applied to remove the apo-protein from the surface, with the thiolated heme derivative remaining on the surfaces. Apo-protein was again introduced to the same surface for the reconstitution of holo-cyt.b562. The success of the association and dissociation reactions between apo-protein and tethered heme molecules on the surfaces was confirmed by the optical thickness changes.

Thin-film formation of proteins and its characterization have been widely studied in both academic and industrial research laboratories.[1–13] Manipulation of proteins by physical or chemical methods is an important aspect in protein engineering. Future bioelectronic devices will require modifications of native components in order to interface them with technical structures, e.g., electrodes, optical transducers and microchannels, and to get acclimated to non-native functional environments. In order to contribute to the development of biosensor application, we report here one method to prepare surface-immobilized protein films. We have chosen cytochrome b_{562} (cyt.b562),[3,14–21] which is one of the heme proteins, as a model protein for the fabrication of protein monolayers and their application to bioelectronic devices. Heme proteins are a particularly interesting class due to the unique electronic and optical properties associated with the porphyrin-based prosthetic group. Cyt.b562 is a small (M_r 12000) water-soluble protein found in *Escherichia coli*, consisting of 106 amino acid residues.[14] The structure of the *Escherichia coli* cyt.b562 has been revealed by X-ray crystallography to a resolution of 0.25 nm. Results showed that cyt.b562 consists of four α-helices.[15,16] The prosthetic group of cyt.b562, protoheme (heme), is noncovalently bound and is ligated to the polypeptide chain through methionine 7 on the *N*-terminal helix and histidine 102 on the *C*-terminal helix. Therefore, this heme can be easily extracted from the holo-protein, modified with a synthetic-chemical procedure, and then easily reconstituted with the original apo-protein in vitro.[3,17] For example, we could synthesize heme derivative with octadecyl chains and reconstitute holo-cyt.b562 from apo-cyt.b562 (AC-b562) and its modified heme. We reported the monolayer formation of its reconstituted cyt.b562 on a water surface.[3]

Although the reconstitution reaction in solution was reported,[3,17] the direct visualization of this reconstitution process of the heme proteins in solution is not possible. However, via attachment of the heme molecule to the surface,[22–26] we have a possibility to visualize this reconstitution process (recognition process between the heme group and the peptide chain) by the use of microscopic tools such as scanning force microscopes. Figure 1 schematically represents the reconstitution reaction of cyt.b562 on a gold substrate. The basic concept is the use of the self-assembling method. Self-assembled monolayer (SAM) formation of organosulfur compounds on metal surfaces have been widely studied because of their extensive applications in molecular technologies.[27–32] Thiols and disulfides co-

Present Address: Analytical Sciences Laboratory, Research & Development Center, Hitachi Chemical Co., Ltd., 48 Wadai, Tsukuba-shi, Ibaraki 300-4247

Present Address: Department of Photonics Materials Science, Chitose Institute of Science and Technology, 758-65 Bibi, Chitose, Hokkaido 066-8655

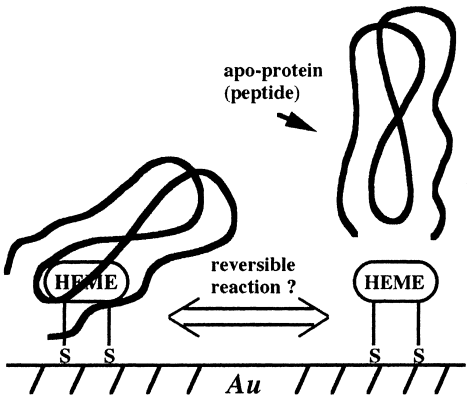

Fig. 1. Schematic representation of the folding reaction of cyt.b562 on a gold surface.

valently adsorb onto gold surfaces through a sulfur-gold linkage, leading to the formation of highly ordered SAMs. As one can see in Fig. 1, once the thiolated-heme derivative is fixed on the gold surface via gold-sulfur linkage, association or dissociation reactions of the peptide chain with the heme moiety can occur and its process can be visualized. There are two ways to have this kind of system. One is to start from the left side of Fig. 1. Firstly, the reconstituted cyt.b562 (RC-b562) which is reconstituted from AC-b562 and thiolated-heme derivative in solution is directly adsorbed, and then the dissociation and association reactions of the peptide chain are observed. The other option is to start from the right side of Fig. 1. After the formation of heme monolayer on the gold surface, the association reaction happens as a second step. But, in this case, an appropriate distance between the two tethered heme groups is required in order to accommodate the peptide chain, which is larger than the heme derivatives. To generate such surfaces, however, is not an easy task. Therefore, we have decided to start the experiment from the left side of Fig. 1: that is, firstly facilitate the direct adsorption of the protein; secondly, induce the dissociation reaction of the peptide; thirdly, observe the recognition (association) reaction. This report will be the first step for our final goal to visualize molecular recognition. In this paper, we will introduce how cyt.b562 can be immobilized on the surface; then we will describe how the peptide will be detached and finally reconstituted by the association reaction between the remaining heme on the surface and the peptide chains. Originally native cyt.b562 (NC-b562) has no cysteine residue in the peptide chain, which is a great advantage in using this protein for the SAM formation on gold surfaces and for anisotropic orientation.

We have utilized surface plasmon resonance spectroscopy (SPS) to detect chemical reactions occurring on the gold surface. SPS is a useful and powerful analytical technique for the in situ investigation of the adsorption phenomenon from solution to solid surfaces.[33,34] SPS is an optical technique that senses the refractive index of a medium near the deposited metal on a glass substrate. This method allows for the direct monitoring of the kinetics of the interactions between an adsorbate and a surface site in real time. The observation of a resonance-curve shift of SPS during the monolayer formation on a surface gives information about the surface concentration of the adsorbate. SPS has been used for the detection of protein adsorption. Mrksich et al. demonstrated that SPS can be used to measure the nonspecific adsorption of proteins to alkanethiolate SAMs on gold in situ and in real time.[5] Spinke et al. have also employed SPS for the detection of the assembling reaction of mono- and multi-layer protein films at solid/liquid interface, using the strong interaction between biotin and streptavidin.[8,9]

Experimental

Materials and Sample Preparations. Hemin (iron protoporphyrin IX chloride) was purchased from Funakoshi, Japan. 2,2′-dithiobis(ethylamine) dihydrochloride was obtained from Tokyo Kasei, Guanidine hydrochloride (GdnHCl) from Fluka, and Proteinase K from Merck. All other chemicals were from Kanto Chemical. All chemicals were used without further purification. Gold (99.999%) was purchased from Furuya Metal, and the glass slides (LaSFN9) were from S & J Trading Inc., USA.

Thiolated-heme derivative was synthesized from hemin chloride and 2,2′-dithiobis(ethylamine) dihydrochloride. The synthetic procedure was reported before.[22] The structure of the heme derivative used in this study is shown in Fig. 2.

Cyt.b562 was obtained from *Escherichia coli* strain TB-1 harboring pNS 207 grown in LB medium.[35] The harvested cells were resuspended in 10 mM Tris-HCl/1 mM EDTA, pH 8.0, buffer and were subjected to a chloroform extraction.[36] The supernatant solution containing cyt.b562 was titrated to pH 4.55 and was stirred for a minimum of 30 min at 4 °C. The precipitate was removed by centrifugation, and the supernatant solution was loaded onto a carboxymethylcellulose ion-exchange column chromatograph (Whatman) equilibrated with 50 mM KH_2PO_4/0.1 mM EDTA, pH 4.55, buffer and eluted with a salt gradient of 0–200 mM KCl. The eluted fractions were concentrated, and then applied to a Sephadex G-50 gel filtration column chromatograph (Pharmacia) equilibrated with a buffer containing 50 mM Tris-HCl/0.1 mM EDTA, pH 8.0. The protein, cyt.b562, used in this study had an absorption ratio of 6.1 for A_{418}/A_{280} in the oxidized state; this value is an index of the purification.

The AC-b562 was prepared at 4 °C using the butanone extraction method.[37] Typically, the cyt.b562 solution was titrated to pH

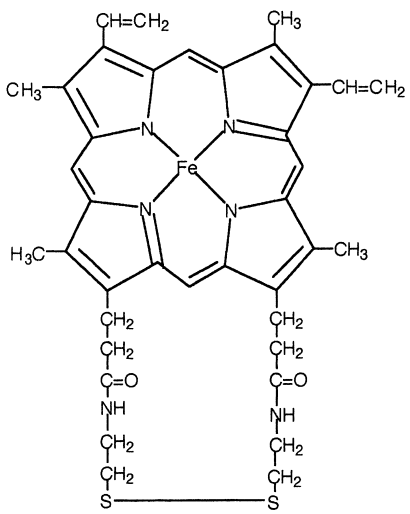

Fig. 2. Structure of heme derivative used in this study.

2.0 by adding 1.0 M of pre-cooled HCl. An equal volume of butanone, pre-cooled to 4 °C, was used repeatedly to extract the red heme until the butanone layer became colorless. The AC-b562 was dialyzed against pure water (Milli Q, Millipore Milli Q system) for 4 days with several pure water changes. The obtained AC-b562 contained no holo-protein, as indicated from the absence of the Soret band. The reconstitution of holo-protein from AC-b562 and a native heme can be achieved by reaction in an alkaline pH buffer.[17] Since the heme derivative is insoluble in water, a mixture of dimethyl disulfoxide and Tris-buffer (50 mM Tris-HCl, 0.1 mM EDTA, pH 8.0) was used as the solvent for the reconstitution reaction.[3] We have checked the optimal conditions for the reconstitution reaction and found that 50% of dimethyl disulfoxide was best. After the reconstitution reaction, the holo cyt.b562 solution was dialyzed against Milli Q water, centrifuged, concentrated, and then purified with a Sephadex G-50 gel filtration column chromatograph equilibrated with buffer containing 50 mM Tris-HCl/0.1 mM EDTA, pH 8.0. All protein solutions, NC-b562, RC-b562, and AC-b562, were kept at 4 °C and dialyzed just before use for the required buffer ingredient.

Glass slides (LaSFN9) were cleaned in 5% Extran (Merck) in Milli Q water, rinsed with Milli Q water carefully, and then cleaned in ethanol. The slides were then dried in a stream of nitrogen and placed in an Edwards Auto 360 evaporator. A gold film of 50 nm thickness was deposited and used for SPS measurement. SAMs for SPS measurements were formed by applying known concentrations of the solution into an SPS flow cell equipped with gold substrates.

The protein molecules were adsorbed onto either the bare gold substrate or the pre-modified gold surface with 2,2′-dithiodiacetic acid (DTDAA), which was used as a surface modifier. Such a modified layer is normally used to avoid structural denaturation of adsorbed protein.

SPS Measurement. SPS measurements were carried out using the experimental set-up shown in Fig. 3(A).[33,34] A temperature-controlled flow cell was used. The volume of the flow cell was 0.3 cm^3 and flow rate was fixed at 0.5 cm^3 min^{-1}. A 2.5 cm^3 volume of solution was typically introduced to the flow cell (5 min) and then flow was stopped. The intensity change was continuously monitored. In this Kretschmann configuration,[38] the gold coated glass substrates were optically matched to the base of a 90 ° LaSFN9 glass prism (n = 1.85 at λ = 632.8 nm) using an index matching fluid. This allows us to excite plasmon surface polaritons at the metal-dielectric interface, upon total internal reflection of the laser beam (HeNe, λ = 632.8 nm, power 5 mW) at the prism base. By varying the angle of incidence of the laser beam, θ, a plot of reflected intensity as a function of this angle of incidence is obtained, similar to that shown in Fig. 3 (B). The reflected intensity shows a sharp minimum at the resonance angle, θ_1. From the Fresnel fit to the resonance curve for a bare gold surface (line in Fig. 3 (B)), the thickness of the gold film is obtained.[39,40] Adsorption of a thin layer onto the gold surface typically shifts the resonance position to higher angles, from θ_1 to θ_2. Fitting to this second curve determines the optical thickness of the adsorbed layer, from which the geometrical thickness is obtained by assuming a full coverage of adsorbate on the surface and a particular value for the refractive index of adsorbate.[39,40] We have chosen to evaluate our data using one refractive index (n = 1.5) for all the compounds; such a substitution is often adopted for organic thin layers having no absorption bands in the considered range of wavelength.[8] Adsorption processes occurring at the gold interface can

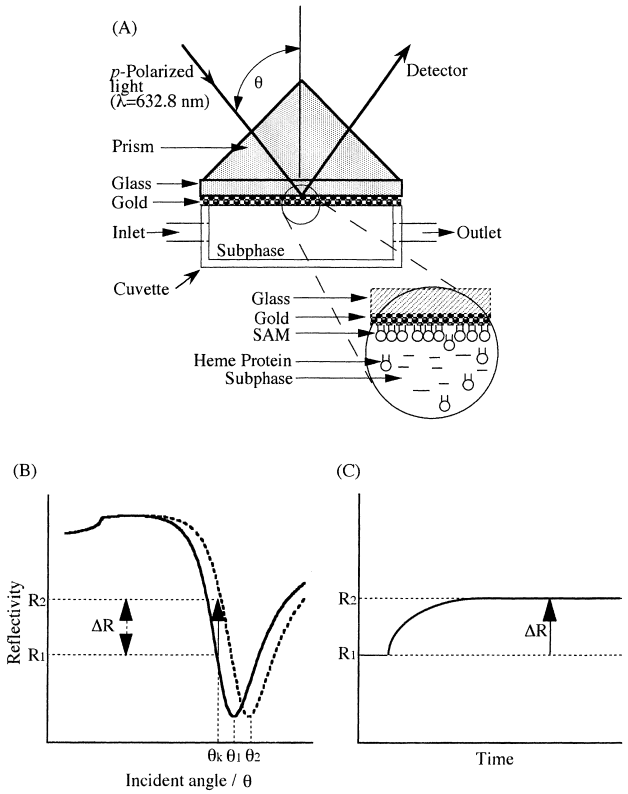

Fig. 3. (A) A schematic diagram of the experimental set-up used for the surface plasmon characterization of monolayers and their formation. (B) A schematic reflectivity versus angle curve obtained with the surface plasmon spectrometer. The angle, θ_1, at the minimum of the reflected intensity is obtained for a bare gold surface, while the angle, θ_2, is obtained after a monolayer is adsorbed on the gold surface. (C) A schematic reflectivity versus adsorption time curve obtained with the surface plasmon spectrometer. The layer formation can be followed in situ by monitoring the reflected intensity at an angle, θ_k, in (B).

be followed in real time, as shown in Fig. 3 (C), by selecting an appropriate angle of incidence, θ_k, and monitoring the reflected intensity as a function of time. Typically, R_1 and R_2 correspond to the thickness of zero and that of adsorbed layer, respectively. Therefore, we can convert the change in the reflected intensity to that in the thickness. In this paper, we discuss the relative change in thickness, because we know neither the refractive index of the protein monolayer nor the surface coverage of proteins on gold surfaces. The arrows in the figure indicate the starting point of the rinsing with the same solvents as were used for the adsorption. Rinsing was performed in order to peel off the second layer that was physically adsorbed.

Results and Discussion

First, the adsorption of the RC-b562 on a gold surface was compared to that of NC-b562. DTDAA was used as a surface modifier in order to avoid denaturation of protein molecules on the gold surface. In order to check the effect of the use of this surface modifier, the protein molecules were adsorbed onto either the bare gold substrate or the pre-modified surface with DTDAA.

The adsorption processes and the final thickness of the protein monolayer were followed in situ by SPS and are shown in Fig. 4. Curve (A) shows the adsorption behavior of DTDAA onto the gold substrate. Curves (B) and (D) show the adsorption behavior of the NC-b562 on DTDAA-modified and on the bare gold substrates, respectively. On the other hand, curves (C) and (E) show the adsorption behaviors of RC-b562. The layer thickness for all samples changed quickly with a steep slope at the beginning of the adsorption, showing the high affinity of the samples to the surfaces, and then reached saturation in thickness within ca. 60 min. The signal decreases after arrows indicate the washout of non-specific binding adsorbates. The thickness of DTDAA (curve A) was about 1.0 nm, which is reasonable, taking into account its structure (chain length). The thickness of NC-b562 on a bare gold substrate (curve D) was about 1.6 nm after rinsing. When NC-b562 adsorbed on DTDAA monolayer, the combined thickness of the two layers, NC-b562 and DTDAA, was about 3.0 nm (curve B). If we assume that DTDAA molecules do not desorb when covered by NC-b562 and that NC-b562 molecules do not denature on top of DTDAA-supported monolayer, we can evaluate the thickness of NC-b562 monolayer on DTDAA as 2.0 nm. This assumption is supported by published reports that studied protein adsorption on modified surfaces by electrochemical methods.[10–13,41] As mentioned above, the protein shape of cyt.b562 is an ellipsoid of revolution with a major axis of 5.0 nm and a minor axis of 2.5 nm. If NC-b562 molecules adsorb sideways on DTDAA monolayer, the thickness of NC-b562 should be 2.5 nm. On the other hand, the thickness of NC-b562 on a bare gold substrate (curve D) was about 1.6 nm, which was smaller than that adsorbed on DTDAA monolayer. This is probably because the protein molecules are denatured and extended sideways. When RC-b562 adsorbed on DTDAA monolayer, the combined thickness of the two layers, RC-b562 and DTDAA, was about 4.0 nm after the rinsing (curve C). As mentioned above, the shape of cyt.b562 is an ellipsoid of revolution. Here we calculated the direction of the branch in the heme molecules from the data of three-dimensional structure of NC-b562 by a computer simulation. The angle between the major axis of ellipsoid and the direction of branch in the heme molecules was 55 degrees.[3] The heme molecule is noncovalently bound to the apo-protein (peptide chain) and it is ligated to the apo-protein through methionine 7 and histidine 102. Therefore, the angle of the heme face should be fixed against the major axis of the ellipsoid (protein molecule). If we assume that two side chains in the heme molecule orient normal to the gold surface, the RC-b562 has to tilt with a certain angle to it. Thus, the theoretically obtained thickness of RC-b562 on the gold substrate is 4.5 nm, which is in good agreement with the experimentally obtained thickness, 4.0 nm. Here we discussed with the assumption that the desorption of DTDAA with the adsorption of RC-b562 (replacement) occurs, that is, the RC-b562 adsorbs on gold surfaces through the gold-sulfur linkage. This assumption is probably appropriate, because the curves (B) and (C) should be overlapped if the replacement reaction did not occur. There are some reports that studied the competitive and replacement reactions of thiolated compounds on the gold surface. If two different compounds, both of which have sulfur in the molecules, competitively adsorb onto the surface, the bigger molecules preferably adsorb on the surface.[42,43] When the RC-b562 adsorbs on the gold substrate with the desorption of DTDAA molecules, RC-b562 are thought to keep the native structure from the points of the thickness (see; Fig. 10 (b)) with the help of remaining DTDAA molecules on the surface. On the other hand, the thickness of RC-b562 on a bare gold substrate (curve E) was about 2.2 nm, which was smaller than the value obtained in curve (C) and bigger than that obtained in curve (D). With the comparison to curve (C), the protein molecules are probably denatured, but with comparison to curve (D), the protein has still maintained the partial original structure (tilted structure) contributed by the direct adsorption of sulfur moiety in the heme molecule to the gold surface.

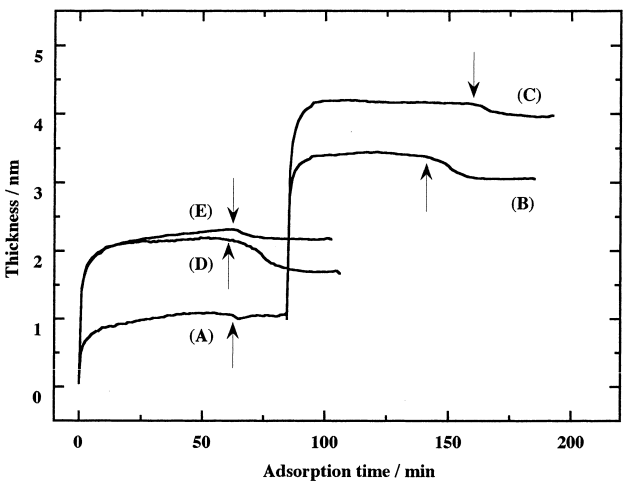

Fig. 4. In situ surface plasmon kinetics measurements of protein adsorption. (A) 750 μM of DTDAA in ethanol was adsorbed on a bare gold surface, (B) 50 μM of NC-b562 in Milli Q was adsorbed on a gold surface pretreated with DTDAA as shown in line (A), (C) 50 μM of RC-b562 in Milli Q was adsorbed on a gold surface pretreated with DTDAA as shown in line (A), (D) 50 μM of NC-b562 in Milli Q was adsorbed on a bare gold surface, and (E) 50 μM of RC-b562 in Milli Q was adsorbed on a bare gold surface. Each solution was introduced into a flow cell coupled to the surface plasmon spectrometer at 23 °C. Arrows show the start of rinsing.

The influence of the initial solution concentration on the adsorption kinetics and layer thickness was measured by SPS for RC-b562 solutions ranging from a concentration of 1 μM to 50 μM. The result is shown in Fig. 5. The adsorption profiles show that the surface coverage of adsorbate increases up to solution concentrations of 10 μM, above which the surface coverage of adsorbate reaches a maximum and the initial concentration does not significantly influence the final thickness of the adsorbed protein molecules. This concentration dependence on the adsorbed amount is frequently observed for the adsorption of thiolated compounds.[22,27,31] Therefore, we used 10 μM as the initial concentration for the samples to ensure the full coverage of adsorbate in all subsequent experiments.

Figure 6 shows the results of the dissociation reactions of cyt.b562 adsorbed on a gold surface. In order to keep the heme molecules on the surface and to remove only the peptide

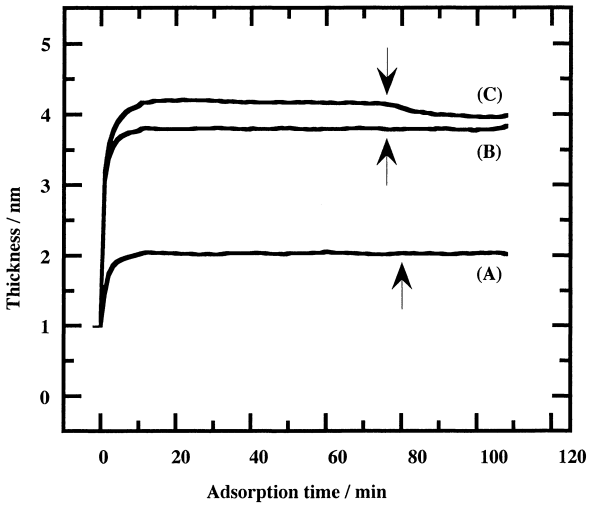

Fig. 5. Initial concentration dependence on RC-b562 adsorption kinetics measured by in situ surface plasmon spectrometer at 23 °C. (A) 1 μM, (B) 10 μM, and (C) 50 μM of protein solution were introduced into the flow cell. The substrates were pre-covered with DTDAA. Arrows show the start of rinsing.

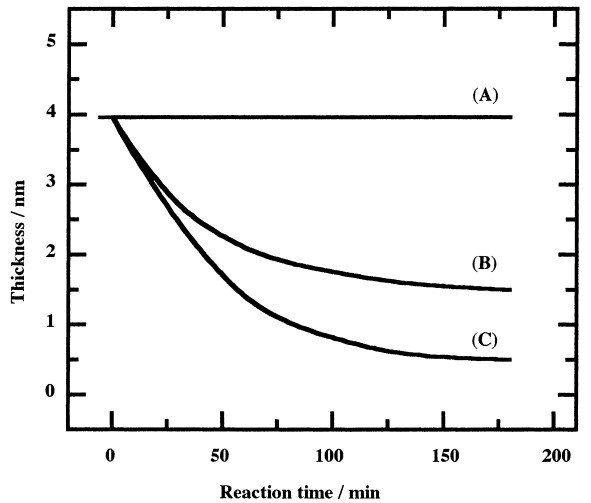

Fig. 6. Dissociation reaction of RC-b562 adsorbed on gold surfaces. (A) 4 M-GdnHCl, pH 8.0, 6 M-GdnHCl, pH 8.0, 13.5 μM-proteinase K, pH 8.0, 13.5 μM-proteinase K with 3 M-GdnHCl, pH 8.0, (B) 4 M-GdnHCl, pH 5.0, and (C) 8 M-GdnHCl, pH 5.0, were reacted with RC-b562 adsorbed on gold surfaces pretreated with DTDAA in a flow cell of surface plasmon spectrometer at 23 °C. 50 mM of phosphate, pH 5.0, and 50 mM of Tris-HCl, pH 8.0, were used as buffers.

chains (AC-b562) away from the surfaces, we studied the dissociation reactions under several different conditions. GdnHCl, known as a denaturing agent, and proteinase K, known to digest enzyme by hydrolysis, were employed. Curve (A) shows the thickness change if GdnHCl, or proteinase K, or both are applied to the system at pH 8.0. Under these conditions, no significant change in thickness was observed. Figures 6 (B) and (C) show the thickness change when 4 M and 8 M GdnHCl solution at pH 5.0 were introduced respectively. Obviously these concentrations of GdnHCl in the solutions at pH 5.0 could remove the peptide chain. Wittung-Stafshede et al. studied the structural unfolding of cyt.b562 in solutions of various GdnHCl concentrations.[21] They reported that the oxidized cyt.b562 is fully denatured at 2 M GdnHCl, whereas the reduced cyt.b562 did not unfold below 6 M GdnHCl, but denatured at 8 M GdnHCl. Our results show the different dissociation behavior at the concentrations of 4 M and 8 M of GdnHCl. There are two ways to explain this difference. One is the oxidized and reduced cyt.b562 molecules co-exist on the gold surface. In this case, at the concentration of 4 M GdnHCl, only the oxidized cyt.b562 molecules denatured. The other is that the cyt.b562 molecules stabilized on the gold surface with the help of surface modifier, DTDAA. Therefore, the required GdnHCl concentration shifted from 2 M to higher concentration above 4M toward the protein unfolding, even if all the cyt.b562 molecules are oxidized. When a pure SAM of either heme or DTDAA was rinsed with 8 M of GdnHCl solution, GdnHCl did not remove anything from the surfaces (data not shown). This means that, under the experimental conditions employed in this study, GdnHCl removed the peptide only, and both heme derivative and DTDAA molecules remained on the gold surfaces after the dissociation reactions. NC-b562 has a compact structure given by the association between heme and peptide. AC-b562 has a much looser structure because of the lack of the heme. This is the reason why proteinase K was not able to hydrolyze the peptide chain on the surfaces at pH 5.0. As described in the experimental section, heme molecules are normally extracted under acidic conditions in the presence of organic solvents such as ketones. The reason why acidic conditions are frequently used is that the pK_a of the imidazole ring of Histidine 102 in the peptide chain is about 6.0, weakening the binding between the heme and the peptide below pH 6.0 (it is not dissociated; this cyt.b562 is reported to be stable under pH conditions ranging from pH 2 to pH 12.).

Figure 7 shows the thickness change when an AC-b562 solution at pH 8.0 was applied to the gold surface on which the

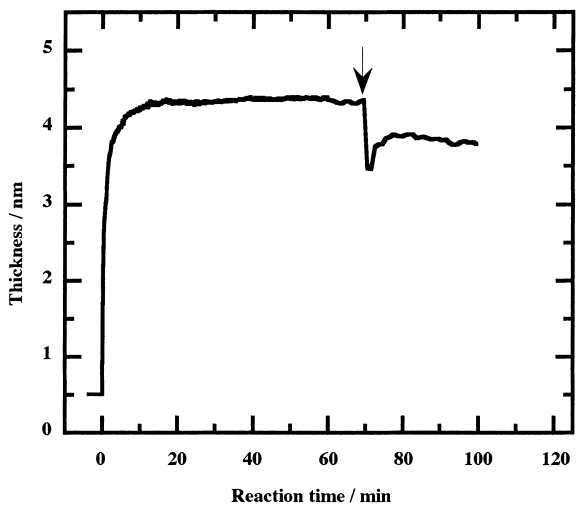

Fig. 7. Reconstitution (association) reaction of the remaining heme with 10 μM of AC-b562 in 50 mM Tris-HCl, pH 8.0 studied by in situ surface plasmon spectroscopy at 23 °C.

thiolated heme molecules remain. The layer thickness increased with a steep slope at the beginning of adsorption, showing the high affinity of AC-b562 to the surfaces, and then continued with a slower adsorption processes. Although we have no direct evidence about structural information, initial adsorption stage is composed from the physical adsorption of AC-b562 on the surface and consequent reconstitution reactions of AC-b562 with the remaining heme molecules through the molecular recognition. The net increase in thickness by the association reactions was about 3.3 nm, which is almost the same as the decrease shown in Fig. 6 (C). In order to confirm that the increase in this thickness is due to the folding process and not only caused by physical adsorption of the AC-b562 to the surfaces, we studied the adsorption behaviors of AC-b562 on either a bare gold surface or on a DTDAA modified surface; the results are shown in Figs. 8 (A) and (B), respectively. The thickness of AC-b562 directly adsorbed on the bare gold surface was about 1.3 nm, whereas that adsorbed to a DTDAA-modified surface was about 1.5 nm, if we subtract the initial thickness of the DTDAA monolayer. This adsorption behavior of AC-b562 on the surfaces is the same as that of NC-b562 shown in Figs. 4 (B) and (D). Here we again suppose that no desorption of DTDAA molecules accompanies the adsorption of AC-b562. The thickness increase obtained in Fig. 8 was much smaller than that obtained in Fig. 7. Therefore, we can conclude that the thickness increase obtained in Fig. 7 was due to the recognition reaction between the heme groups and AC-b562, leading to final association.

Figure 9 summarizes the whole kinetics of the protein adsorption, dissociation and re-association reactions of cyt.b562 under optimum conditions found through this study. Curve (A) shows the adsorption kinetics of the surface modifier, DTDAA, which was effective to precover the gold surface before the protein adsorption, in order to avoid the structural denaturation of the protein molecules. Curve (B) gives the adsorption kinetics of RC-b562, with a final thickness of about 4.0 nm. When we introduced 8 M of GdnHCl under acidic conditions, the peptide chain (AC-b562) was effectively removed, but the heme groups remained on the surfaces, as shown in curve (C). Finally, curve (D) gives the adsorption kinetics of AC-b562 onto the gold surface on which the thiolated heme molecules remain. Its final thickness after the association reaction was about 3.8 nm. This value is almost the same as the initial thickness of RC-b562 adsorbed on the DTDAA surface.

Figure 10 represents a schematic drawing of the adsorption/

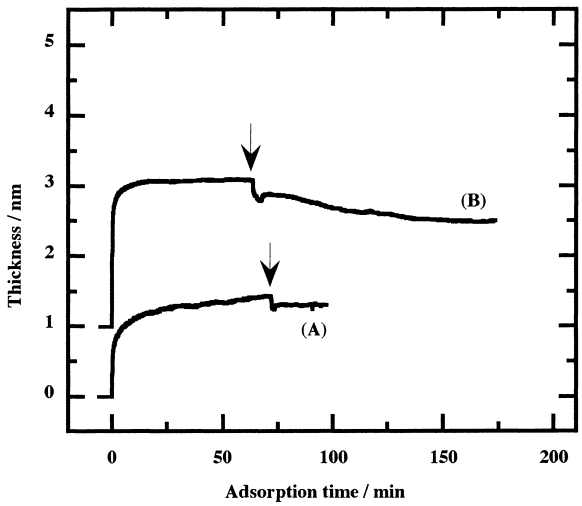

Fig. 8. In situ surface plasmon kinetics measurements for AC-b562 adsorption at 23 °C. 10 μM of AC-b562 in 50 mM TrisHCl, pH 8.0 was adsorbed either (A) on a bare gold surface or (B) on a gold surface pretreated with DTDAA.

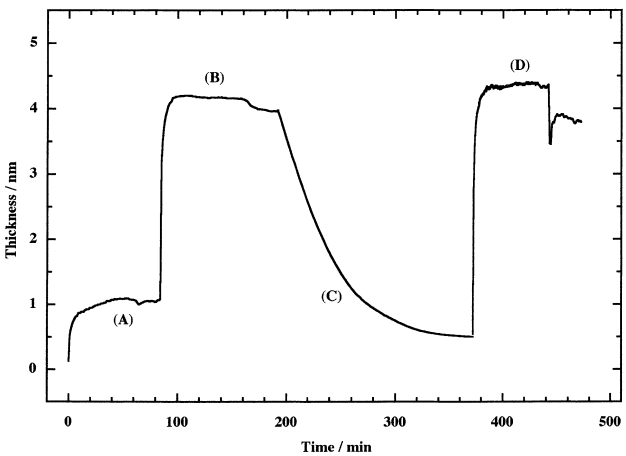

Fig. 9. Whole kinetics of adsorption, dissociation, and reconstitution reactions for cyt.b562 on gold surfaces. (A) adsorption of 750 μM of DTDAA in ethanol on a bare gold surface, (B) adsorption of 10 μM of RC-b562 in Milli Q on the surface of (A), (C) dissociation reaction with 8 M of GdnHCl, pH 5.0, at the surface of (B), and (D) reconstitution reaction with 10 μM of AC-b562 in 50 mM TrisHCl, pH 8.0.

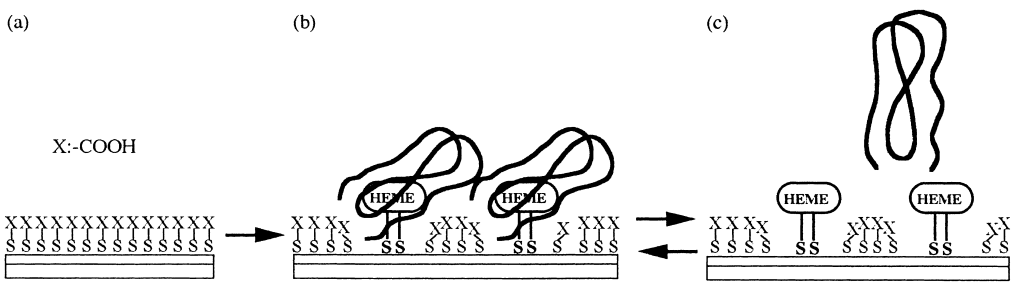

Fig. 10. Schematic drawing of the association and dissociation reactions of cyt.b562 on gold surfaces.

reconstitution reactions on the surface given in Fig. 9. Figures 10 (a), (b), and (c) show the surface structures of DTDAA (Fig. 9 (A)), RC-b562 (Figs. 9 (B) and (D)), and the remaining heme molecules on surfaces with the AC-b562 in solution (near the surface), respectively. The association/dissociation reaction between bound (Fig. 10 (b)) and free (Fig. 10 (a)) apo-protein and the surface-attached heme is reversible, as was shown in this study.

In further studies, we will focus on the electron-transfer properties between the heme as prosthetic group in protein and the electrode. The spacer length between heme moiety and the gold surface is very important. Therefore, we will publish elsewhere this chain length dependence and also the structural information of cyt.b562 adsorbed on the gold surfaces.

We would like to thank Prof. S. G. Sligar (University of Illinois, USA) for providing us with the over-expressed *Escherichia coli* strain and also Prof. H. Rigsdorf (University of Mainz, Germany) for helpful discussions.

References

1 T. Furuno, H. Sasabe, and A. Ikegami, *Ultramicroscopy*, **70**, 125 (1998).
2 K. Nagayama, *Adv. Biophys.*, **34**, 3 (1996).
3 K. Kobayashi, T. Nagamune, T. Furuno, and H. Sasabe, *Bull. Chem. Soc. Jpn.*, **72**, 691 (1999).
4 K. Kobayashi, N. Ishii, H. Sasabe, and W. Knoll, *Biosci. Biotechnol. Biochem.*, **65**, 176 (2001).
5 M. Mrksich, G. B. Sigal, and G. M. Whitesides, *Langmuir*, **11**, 4383 (1995).
6 E. K. Schmidt, T. Liebermann, M. Kreiter, A. Jonczyk, R. Naumann, A. Offenhäusser, E. Neumann, A. Kukol, A. Maelicke, and W. Knoll, *Biosens. Bioelectron.*, **13**, 585 (1998).
7 L. Häussling, H. Ringsdorf, F.-J. Schmitt, and W. Knoll, *Langmuir*, **7**, 1837 (1991).
8 J. Spinke, M. Liley, H.-J. Guder, L. Angermaier, and W. Knoll, *Langmuir*, **9**, 1821 (1993).
9 J. Spinke, M. Liley, F.-J. Schmitt, H.-J. Guder, L. Angermaier, and W. Knoll, *J. Chem. Phys.*, **99**, 7012 (1993).
10 H.-G. Hong, M. Jiang, S. G. Sligar, and P. W. Bohn, *Langmuir*, **10**, 153 (1994).
11 L. L. Wood, S.-S. Cheng, P. L. Edmiston, and S. S. Saavedra, *J. Am. Chem. Soc.*, **119**, 571 (1997).
12 L. Jiang, A. Glidle, C. J. McNeil, and J. M. Cooper, *Biosens. Bioelectron.*, **12**, 1143 (1997).
13 D. Kröger, M. Liley, W. Schweck, A. Skerra, and H. Vogel, *Biosens. Bioelectron.*, **14**, 155 (1999).
14 E. Itagaki and L. P. Hager, *J. Biol. Chem.*, **241**, 3687 (1966).
15 F. S. Mathews, P. H. Bethge, and E. W. Czerwinski, *J. Biol. Chem.*, **254**, 1699 (1979).
16 P. C. Weber, F. R. Salemme, F. S. Mathews, and P. H. Bethge, *J. Biol.Chem.*, **256**, 7702 (1981).
17 E. Itagaki, G. Palmer, and L. P. Hager, *J. Biol. Chem.*, **242**, 2272 (1967).
18 G. R. Moore, R. J. P. Williams, J. Peterson, A. J. Thomson, and F. S. Mathews, *Biochim. Biophys. Acta*, **829**, 83 (1985).
19 P. D. Barker, J. L. Butler, P. de Oliveira, H. A. O. Hill, and N. I. Hunt, *Inorg. Chim. Acta*, **252**, 71 (1996).
20 P. Wittung-Stafshede, H. B. Gray, and J. R. Winkler, *J. Am. Chem. Soc.*, **119**, 9562 (1997).
21 P. Wittung-Stafshede, J. C. Lee, J. R. Winkler, and H. B. Gray, *Proc. Natl. Acad. Sci. U. S. A.*, **96**, 6587 (1999).
22 K. Kobayashi, S. Imabayashi, K. Fujita, K. Nonaka, T. Kakiuchi, H. Sasabe, and W. Knoll, *Bull. Chem. Soc. Jpn.*, **73**, 1993 (2000).
23 T. Lötzbeyer, W. Schuhmann, and H.-L. Schmidt, *J. Electroanal. Chem.*, **395**, 341 (1995).
24 F. Arifuku, T. Saeki, and H. Kurihara, *Fukuoka Univ. Sci. Reports*, **23**, 63 (1993).
25 J. Zak, H. Yuan, M. Ho, K. Woo, and M. D. Porter, *Langmuir*, **9**, 2772 (1993).
26 P. Wagner, M. Hegner, H.-J. Güntherodt, and G. Semenza, *Langmuir*, **11**, 3867 (1995).
27 A. Ulman, *Chem. Rev.*, **96**, 1533 (1996).
28 H. Takiguchi, K. Sato, T. Ishida, K. Abe, K. Yase, and K. Tamada, *Langmuir*, **16**, 1703 (2000).
29 K. Fujita, M. Hara, H. Sasabe, W. Knoll, K. Tsuboi, K. Kajikawa, K. Seki, and Y. Ouchi, *Langmuir*, **14**, 7456 (1998).
30 K. Tamada, J. Nagasawa, F. Nakanishi, K. Abe, T. Ishida, M. Hara, and W. Knoll, *Langmuir*, **14**, 3264 (1998).
31 K. Fujita, N. Bunjes, K. Nakajima, M. Hara, H. Sasabe, and W. Knoll, *Langmuir*, **14**, 6167 (1998).
32 K. Uosaki, T. Kondo, X.-Q. Zhang, and M. Yanagida, *J. Am. Chem. Soc.*, **119**, 8367 (1997).
33 W. Knoll, *MRS Bull.*, **XIV**, 29 (1991).
34 W. Knoll, *Makromol. Chem.*, **192**, 2827 (1991).
35 H. Nikkila, R. B. Gennis, and S. G. Sligar, *Eur. J. Biochem.*, **202**, 309 (1991).
36 G. F. -L. Ames, C. Prody, and S. Kustu, *J. Bacteriol.*, **160**, 1181 (1984).
37 F. W. J. Teale, *Biochim. Biophys. Acta*, **35**, 543 (1959).
38 E. Kretschmann, *Z. Phys.*, **241**, 313 (1971).
39 W. N. Hansen, *J. Opt. Soc. Am.*, **58**, 380 (1968).
40 J. G. Gordon and J. P. Swalen, *Opt. Commun.*, **22**, 374 (1977).
41 T. Sagara, H. Murakami, S. Igarashi, H. Sato, and K. Niki, *Langmuir*, **7**, 3190 (1991).
42 K. Tamada, M. Hara, H. Sasabe, and W. Knoll, *Langmuir*, **13**, 1558 (1997).
43 L. P. Folkers, P. E. Laibinis, G. M. Whitesides, and J. Deutch, *J. Phys. Chem.*, **98**, 563 (1994).